1 Title: Extracellular calcification of *Braarudosphaera bigelowii* deduced from electron

2 microscopic observations of cell surface structure and elemental composition of

3 pentaliths

4

5

6 Kyoko Hagino

7 *Research and Education Faculty, Natural Sciences Cluster, Sciences Unit, Kochi*

8 *University, Akebono-cho 2-5-1, Kochi, 780-8520 Japan*

9 E-mail: hagino@kochi-u.ac.jp

10

11 Naotaka Tomioka

12 *Kochi Institute for Core Sample Research, Japan Agency for Marine-Earth Science and*

13 *Technology, 200 Monobe-otsu Nankoku, Kochi, 783-8502 Japan*

14 E-mail: tomioka@jamstec.go.jp

15

16 Jeremy R. Young

17 *Dept. of Earth Sciences, University College London, Gower St., London WC1E 6BT UK*

18 E-mail: jeremy.young@ucl.ac.uk

19

20 Yoshihito Takano

21 *Nagasaki University, Institute for East China Sea Research, 1-14, Bunkyo-machi,*

22 *Nagasaki, 852-8521, Japan*

23 *National Research Institute of Fisheries Science, Fisheries Research Agency, 2-12-4*

24 *Fukuura, Kanazawa, Yokohama, 236-8648 Japan.*

25 E-mail: ytakano@affrc.go.jp

26

27 Ryo Onuma

28 *Department of Natural History Sciences, Graduate School of Science, Hokkaido*

29 *University, N10W8, Sapporo 060-0810, Japan*

30 E-mail: ronuma@nig.ac.jp

31

32 Takeo Horiguchi

33 *Department of Biological Sciences, Faculty of Science, Hokkaido University, N10W8,*

34   *Sapporo, 060-0810, Japan.*

35   E-mail: horig@mail.sci.hokudai.ac.jp

36

37

38   **Abstract**

39   We have performed morphological and crystallographic studies of *B. bigelowii* using

40   various light and electron microscopy techniques. LM study revealed that *B. bigelowii*

41   has a haptonema, and uses it for adhesion to external substrates. TEM study of

42   pentaliths indicates that the well-known lamina substructure is formed in turn of

43   consistently oriented elongated grains of fine-scale calcite having perfectly identical

44   crystallographic orientation. Cytological study shows that the pentaliths of *B. bigelowii*

45   are surrounded by organic structure consists of a pentalith-substrate and thin layers. The

46   pentalith-substrate underlies the proximal surface of the pentaliths and extends between

47   the sides of the individual pentaliths, it also extends between the five segments forming

48   a pentalith. Thin organic layers, which apparently originate from ridges of

49   pentalith-substrate, cover the distal surface of the trapezoidal segments. The close

50   association between the pentalith-substrate, organic layers, and pentaliths lead us to the

51   hypothesis that the *B. bigelowii* calcifies their pentaliths extracellularly, between the

52 pentalith-substrate and organic layers. Relatively high Mg contents observed from

53 pentaliths supports our hypothesis of extracellular calcification of *B. bigelowii*.

54

55 **Key Words**

56 *Braarudosphaera bigelowii*, calcification, coccolith, coccolithophore, haptonema,

57 haptophyte, nannolith

58

59

60 **1. Introduction ver. 1: started with explanation of Braarudosphaera.**

61 The family Braarudosphaeraceae comprises unicellular coastal phytoplankton and

62 belongs to the Class Prymnesiophyceae, Division Haptophyta (Takano et al., 2006).

63 They are characterized by very distinctive calcareous scales called pentaliths which

64 have pentameral symmetry and are formed of 5 segments with a laminar sub-structure,

65 (e.g. Perch-Nielsen, 1985a, b). The family first appeared in the Early Cretaceous, and

66 *Braarudosphaera bigelowii*, the extant type species of the family, appeared in the Late

67 Cretaceous (e.g. Bown, 1998). Fossils of *B. bigelowii* were usually very rare or absent

68   in marine sediments, however, exceptionally became dominant in specific

69   time-intervals; in the early Danian immediately after the K/Pg mass extinction that

70   eliminated ca. 90% of calcareous nannofossils, and in the Oligocene diversity minimum

71   (e.g. Bown et al., 2004). Thus, *B. bigelowii* is an important species for understanding

72   the calcareous nannofossil assemblages after the extinction events. Extant *B. bigelowii*

73   has not been successfully cultured yet, and its ecological preferences are still unclear.

74   However, progresses of various studies on living *B. bigelowii* as well as that of

75   members of the class Prymnesiophyceae (Division Haptophyta) that includes the family

76   Braarudosphaeraceae in the last decade have unveiled the nature of the

77   Braarudosphaeraceae, as below.

78   The Division Haptophyta is predominantly marine unicellular phytoplankton,

79   characterized by a thread-like organelle, the haptonema, with a unique microtubular

80   cytoskeletal structure, which is inserted between two flagella (e.g. Green and

81   Leadbeater, 1994). The Haptophyta consists of two classes Pavlovophyceae and

82   Prymnesiophyceae. Members of the Pavlovophyceae have two unequal flagella and a

83   non-coiling rudimentary haptonema, while the members of the Prymnesiophyceae have

84   two equal/subequal flagella and a variably developed haptonema (e.g. Edvardsen et al.,

85   2011; Green and Hori, 1994). In the class Prymnesiophyceae, *Chrysochlomulina*

86   possesses coiling haptonema (e.g. Edvardsen et al., 2011), and some *Chrysochromulina*

87   species use the haptonema for adhesion to external substrates (Inouye and Kawachi,

88   1994) and for handling of food (Kawachi et al., 1991).

89   Members of the Prymnesiophyceae have organic and/or mineralized scales on their cell

90   surface, and those which   which produce calcareous scales, are called

91   coccolithophores . (de Vargas et al., 2007) proposed the subclass Calcihaptophycidae

92   for coccolithophores, although it has not yet been confirmed whether the lineages with

93   calcified scales have a monophyletic origin, since the position of the Family

94   Braarudosphaeraceae in the Prymnesiophyceae changes dependant on the analyses

95   (Hagino et al., 2013; Takano et al., 2006).

96   Calcified scales of coccolithophores are roughly classified into three groups;

97   heterococcolith, holococcolith, and nannolith, based on their morphology.

98   Heterococcoliths are formed of a radial array of complex crystal units, while

99   holococcoliths are formed of numerous minute euhedral crystals. Calcareous scales,

100   which do not clearly conform to either the heterococcolith or holococcolith pattern are

101   referred to as nannoliths, with the understanding that this is likely to be a very mixed

102   group (Young et al., 1999; Young et al., 2003). Pentaliths of the Braarudosphaeraceae

103   consists of five segments each of which behaves optically as a single crystal unit but

104   which have a distinctive laminar sub-structure (e.g. Bown, 1998) . The pentaliths do not

105   conform to either the heterococcolith and holococcolith calcification mode, and so are

106   included in the nannolith group (e.g. Young et al., 1999; Young et al., 2003).

107   Haptophytes, including coccolithophores, reproduce asexually by binary fission in both

108   the diploid and haploid phases. Morphology of coccolith drastically changes in their life

109   cycle (e.g. Young et al., 2003). Members of the Coccolithales, Syracosphaerales, and

110   Zygodiscales produce heterococcoliths and holococcoliths in their diploid and haploid

111   phases, respectively. Members of the Noëlaerhabdaceae (Isochrysidales) produce

112   heterococcoliths in the diploid phase, but do not calcify in the haploid phases (e.g.

113   Houdan et al., 2004; Young et al., 2003). Morphological change of *B. bigelowii*

114   accompanying with alternation of life cycle has been partly revealed by molecular

115   phylogenetic study. A sequence from a non-calcifying motile cell culture strain, which

116 was originally identified as *Chrysochomulina parkeae* (Medlin et al., 2008), fell within

117 the *B. bigelowii* clade in a molecular phylogenetic tree based on 18S rDNA sequences

118 (Hagino et al., 2013; Thompson et al., 2012). As a result and following cytological

119 study, *C. parkeae* was determined to be an alternate life-cycle phase of *B. bigelowii*, and

120 *B. bigelowii* has priority over *C. parkeae* in taxonomy (Hagino et al., 2013).

121 Previous studies have revealed that the sites for calcification of heterococcoliths and

122 holococcoliths differ from each other. Calcification of heterococcoliths occurs

123 intracellularly, in the Golgi cisternae or in a special vacuolar system of the endoplasmic

124 reticulum directly connected to the nuclear membrane, and subsequently extruded onto

125 the cell surface (e.g. Drescher et al., 2012; Westbroek et al., 1989). The mechanism of

126 calcification of holococcoliths has not been determined enough yet, although it is

127 thought that calcification occurs extracellularly, and the outermost membrane or

128 'envelope' plays some role in calcification (Rowson et al., 1986). The morphology of

129 pentaliths greatly differs from that of both heterococcoliths and holococcoliths,

130 therefore, it is difficult to infer the site and mechanism of calcification of pentalith from

131 its morphology. Indeed the site and mechanism of calcification of pentaliths is an

132 interesting unsolved question, in particular it is unknown whether the pentaliths form

133 intracelluarly and are transported to the cell-surface or whether they form in situ, and so

134 extracellularly.

135 A possible approach to this is to use coccolith chemistry.   (Cros et al., 2013) compared

136 the elemental composition of heterococcoliths and holococcoliths using energy

137 dispersive spectroscopy (EDS) equipped to secondary electron microscope (SEM).

138 They showed that holococcoliths differ from heterococcoliths in their Mg/Ca ratio, and

139 suggested that this is likely caused by the difference in calcification mechanism. At this

140 moment, there is no information on elemental compositions of pentaliths of the

141 Braarudosphaeraceae.

142 We have not successfully grown *B. bigelowii* in culture yet, and have not observed

143 process of calcification of pentaliths in laboratory. However, we have undertaken SEM

144 and transmission electron microscope (TEM) studies, which reveal a unique cell surface

145 structure on *B. bigelowii* that is likely related to calcification of pentaliths. In this study,

146 we will discuss the formation of pentaliths of *B. bigelowii* based on the cell surface

147   structure morphology, crystallographic texture and elemental composition of the

148   pentaliths.

149

150   **1. Introduction ver. 2; started with explanation of the Haptophytes.**

151   The Division Haptophyta is predominantly marine unicellular phytoplankton,

152   characterized by a thread-like organelle, the haptonema, with a unique microtubular

153   cytoskeletal structure, which is inserted between two flagella (e.g. Green and

154   Leadbeater, 1994). The Haptophyta consists of two classes Pavlovophyceae and

155   Prymnesiophyceae. Members of the Pavlovophyceae have two unequal flagella and a

156   non-coiling rudimentary haptonema, while the members of the Prymnesiophyceae have

157   two equal/subequal flagella and a variably developed haptonema (e.g. Edvardsen et al.,

158   2011; Green and Hori, 1994). In the class Prymnesiophyceae, *Chrysochlomulina*

159   possesses coiling haptonema (e.g. Edvardsen et al., 2011), and some *Chrysochromulina*

160   species use the haptonema for adhesion to external substrates (Inouye and Kawachi,

161   1994) and for handling of food (Kawachi et al., 1991).

162   Members of the Prymnesiophyceae have organic and/or mineralized scales on their cell

163   surface. Some lineages of the Prymnesiophyceae, which produce calcareous scales, are

164   called as coccolithophores collectively. (de Vargas et al., 2007) proposed the subclass

165   Calcihaptophycidae for coccolithophores, although it has not yet been confirmed

166   whether the lineages with calcified scales are monophyletic origin or not, since the

167   position of the Family Braarudosphaeraceae in the Prymnesiophyceae changes

168   dependant on the analyses (Hagino et al., 2013; Takano et al., 2006).

169   Calcified scales of coccolithophores are roughly classified into three groups;

170   heterococcolith, holococcolith, and nannolith, based on their morphology.

171   Heterococcoliths are formed of a radial array of complex crystal units, while

172   holococcoliths are formed of numerous minute euhedral crystals. Calcareous scales,

173   which do not clearly conform to either the heterococcolith or holococcolith pattern are

174   referred to as nannoliths, with the understanding that this is likely to be a very mixed

175   group (Young et al., 1999; Young et al., 2003).

176   Haptophytes, including coccolithophores, reproduce asexually by binary fission in both

177   the diploid and haploid phases. Morphology of coccolith drastically changes in their life

178   cycle (e.g. Young et al., 2003). Members of the Coccolithales, Syracosphaerales, and

179   Zygodiscales produce heterococcoliths and holococcoliths in their diploid and haploid

180   phases, respectively. Members of the Noëlaerhabdaceae (Isochrysidales) produce

181   heterococcoliths in the diploid phase, but do not calcify in the haploid phases (e.g.

182   Houdan et al., 2004; Young et al., 2003).

183   Previous studies revealed that the sites for calcification of heterococcolith and

184   holococcoliths differ from each other. Calcification of heterococcoliths occurs

185   intracellularly, in the Golgi cisternae or in a special vacuolar system of the endoplasmic

186   reticulum directly connected to the nuclear membrane, and subsequently extruded onto

187   the cell surface (e.g. Drescher et al., 2012; Westbroek et al., 1989). The mechanism of

188   calcification of holococcoliths has not been determined enough yet, although it is

189   thought that calcification occurs extracellularly, and the outermost membrane or

190   'envelope' plays some role in calcification (Rowson et al., 1986). (Cros et al., 2013)

191   compared the elemental composition of heterococcoliths and holococcoliths using

192   energy dispersive spectroscopy (EDS) equipped to secondary electron microscope

193   (SEM). They showed that holococcoliths differ from heterococcoliths in their Mg/Ca

194 ratio, and suggested that this is likely caused by the difference in calcification

195 mechanism.

196 The family Braarudosphaeraceae is a unicellular coastal phytoplankton and belongs to

197 the Class Prymnesiophyceae, Division Haptophyta (Takano et al., 2006). They are

198 characterized by five-fold symmetric calcareous scales with laminar structure called

199 pentalith (e.g. Perch-Nielsen, 1985a, b). Pentaliths of the Braarudosphaeraceae consists

200 of five segments each of which behaves optically as a single crystal unit but which have

201 a distinctive laminar sub-structure (e.g. Bown, 1998) . The pentaliths do not conform to

202 either the heterococcolith and holococcolith in structure, and so are included in the

203 nannolith group (e.g. Young et al., 1999; Young et al., 2003).

204 Extant *Braarudosphaera bigelowii*, the type species of the family, have twelve regular

205 pentagonal pentalith each consisting of five trapezoidal segments on their cell surface

206 (Fig. 1). *B. bigelowii* have never been maintained in culture despite many attempts, but

207 its morphological change accompanying with alternation of life cycle has been partly

208 revealed by molecular phylogenetic study. A sequence from a non-calcifying motile cell

209 culture strain, which was originally identified as *Chrysochomulina parkeae* (Medlin et

210   al., 2008), fell within the *B. bigelowii* clade in a molecular phylogenetic tree based on

211   18S rDNA sequences (Hagino et al., 2013; Thompson et al., 2012). As a result and

212   following cytological study, *C. parkeae* was determined to be an alternate life-cycle

213   phase of *B. bigelowii*, and *B. bigelowii* has priority over *C. parkeae* in taxonomy

214   (Hagino et al., 2013).

215   Morphology of pentalith greatly differs from that of heterococcoliths and holococcoliths,

216   therefore, it is difficult to assume the site and mechanism of calcification of pentalith

217   from its morphology. Mechanism of calcification of pentalith is an interesting unsolved

218   question. We have not successfully grown *B. bigelowii* in culture yet, and not observed

219   process of calcification of pentaliths in laboratory. However, we have undertaken SEM

220   and transmission electron microscope (TEM) studies, which reveal a unique cell surface

221   structure on *B. bigelowii* that is likely related to calcification of pentaliths. In this study,

222   we will discuss the formation of pentaliths of *B. bigelowii* based on the cell surface

223   structure morphology, crystallographic texture and elemental composition of the

224   pentaliths.

225

226   **2. Materials and Methods**

227   **2-1. Morphological studies**

228   Sea surface water samples were collected from Tomari Port and offshore Tomari Port,

229   Tottori Prefecture, Japan, on 232 occasions during studies on living coccolithophores

230   from July 2008 through June 2014 (Fig. 1). Detailed information on the samples was

231   given in (Hagino et al., 2015). One or two litre sea-surface water samples were collected

232   using a bucket , prefiltered through a 50-μm plankton net (Sefar Inc. Din-110), and

233   filtered onto Millipore HAWP04700 and/or Whatman 7060– 4710 filters. Twelve filter

234   samples, which were known to contain common *Braarudosphaera bigelowii* from

235   previous study (Hagino et al., 2015), were selected for morphological studies on

236   pentaliths of *B. bigelowii* (Table 1). Small pieces of each filter sample were cut out, and

237   fixed onto an SEM stub using double-sided carbon tape. Samples were coated with gold

238   (Sanyu SC701 MKII), and then examined with an SEM (JEOL JSM 7001F).

239   Three cells of *B. bigelowii*; US15.2-sc11, Furu-sc2, and Furu-SEM1, which were

240   collected from Usuka and Furue Bays, Nagasaki Prefecture, Japan during previous

241   molecular phylogenetic study (Hagino et al., 2009), were used for light and scanning

242 electron microscopic observations of *B. bigelowii* in this study (Table 2). Sea surface

243 water samples were concentrated using a plankton net with 5 μm openings. The cells

244 were isolated using a capillary micropipette in an inverted light microscope (Olympus

245 CKX41), and then photographed by a camera (Olympus DP50) equipped to an upright

246 microscope (Olympus BX50). The side length of pentalith of each isolate was measured

247 on LM images to allow classification of morphotypes of *B. bigelowii.*

248 After the LM study, the specimen Furu-SEM1 was fixed with 4% osmium tetroxide for

249 1 minute, and adhered to poly-L-lysine-coated glass plates, according to the procedure

250 of (Tsutsui et al., 1976). The cell was rinsed with ion-exchanged water for three times,

251 kept in ion-exchanged water for two days, dehydrated in an ethanol series (30, 50, 70,

252 90, 95 and 100%), and then dried using a critical point dryer (Hitachi HCP-2). The cell

253 was coated with gold (Sanyu SC701 MKII), and was examined with SEM (JEOL JSM

254 7001F).

255 The specimen of *B. bigelowii* used for study of the cell surface by TEM was originally

256 collected for studies on molecular phylogeny and morphology *B. bigelowii* (Hagino et

257 al. 2013) from Tomari Port, Tottori, Japan on June 18, 2011 (Table 1). The specimen

258   was found from the same seawater sample that yielded the specimen examined in Fig. 3

259   of (Hagino et al., 2013), and the specimens were prepared for TEM observation together.

260   The methods of preparation for TEM study were fully described in (Hagino et al.,

261   2013).

262

263   **2-2. Crystallographic and elemental analysis of pentaliths.**

264   Two filter samples collected from offshore of Tomari Port prepared with Whatman

265   7060– 4710 filters, which were known to contain sufficient *B. bigelowii* from previous

266   study (Hagino et al., 2015), were selected for the crystallographic and elemental

267   analyses of pentaliths (Table 1). Plankton preserved on surface of filter samples were

268   transferred onto one of two sides of carbon double-sided tapes, and the double-sided

269   tapes with plankton were placed on brass stubs for TEM and SEM-EDS analyses. The

270   samples for crystallographic analyses were coated with gold (Vacuum Device VS-10),

271   and the samples for elemental analyses were coated with platinum (Sanyu SC701 MC),

272   respectively.

273 A specimen of *B. bigelowii* with a complete exotheca of twelve pentaliths, and with no

274 evidence of secondary dissolution or falling off of outer layers, was selected for

275 crystallographic analysis under a focused-ion beam (FIB) apparatus (Hitachi SMI4050)

276 (Appendix 1a). A thin-foil section of the pentalith for TEM observation was prepared

277 by FIB after tungsten coating to avoid Ga-ion damage (Appendix 1b). The interlayers

278 between proximal and distal layers of pentalith were thinned to be ca 180 nm in

279 thickness (Appendix 1c). The thin-foil section was not parallel to the plane of pentalith

280 of *B. bigelowii* due to technical difficulty. Under TEM observation (JEOL

281 JEM-ARM200F), micro-morphology of the calcite grains consisting a segment of

282 pentalith was examined by bright field transmission electron image and high-angle

283 annular dark field scanning transmission electron image (HAADF-STEM), and their

284 crystallographic orientations were examined by selected-area electron diffraction

285 (SAED).

286 Elemental compositions of pentaliths of *B. bigelowii*, coccoliths of *G. oceanica*, *E.*

287 *huxleyi*, and *T. adriatica* encountered under an SEM (Hitachi SU1510) was examined

288 using energy-dispersive spectrometer (EDS) (Horiba EMAX X-act) attached to the

289   SEM. X-ray spectra were acquired at an accelerating voltage of 15 kV for 120 seconds

290   for pentaliths of *B. bigelowii* and heterococcoliths of *G. oceanica* and *T. adriatica*, and

291   for 240 seconds for heterococcoliths of *E. huxleyi*, with 3-8 % of dead time. X-ray

292   intensities in counts of Mg-Kα and Ca-Kα lines in respective spectra were analyzed

293   using the software Horiba EMAX 1.0.

294

295   **3. Results**

296   **3-1. Morphological studies of pentaliths**

297   A total of 57 specimens of *B. bigelowii* were photographed from 12 samples from

298   Tomari Port or offshore Tomari in SEM (Table 1). Side length of pentaliths observed in

299   this study ranged from 5.5-8.0μm, which corresponds to the size range of Intermediate

300   form-B of Hagino et al. (2009). The outermost lamina of each intact pentalith has a

301   smooth surface (topmost pentalith of the Fig. 2a). The inner laminae, which were

302   exposed by detachment of distal laminae, always have fine grooves (Figs 2a and 2b).

303   Direction of the grooves is almost perfectly consistent, as indicated by double-headed

304   arrows on Figs. 2a and 2b. The fine grooves appear to run parallel to the

305   crystallographic c-axis of the calcite crystal units as estimated by previous study

306   (Appendix 2, Kameo and Furukawa, 2007).

307   The intensity of calcification of the different pentaliths covering a single cell was

308   consistent on all the observed cells, but varied between cells even from the same

309   seawater sample. Pentaliths of lightly calcified specimens are often concave (Figs 2c-d).

310   A pentalith with incomplete layers was found in the sample collected from st. 1 of

311   Tomari Port in June 20, 2010 (Fig. 2e). In this pentalith, calcification mainly occurred

312   around the outline of the pentalith and along the contact surfaces between the segments

313   (= pentalith-substrate, which is defined in the section 3-3). The central part of four of

314   the five segments was hollow. Each segment was composed of multiple incomplete

315   layers (arrow on Fig. 2e). A specimen without any calcareous pentaliths but with

316   pentagonal impressions on its cell surface (Fig. 2f) was found in a sample (st.1, June 21,

317   2010), which yielded many well-calcified specimens.

318

319   **3-2. Light microscopic studies of living *B. bigelowii***

320   Side length of the pentalith of the isolates Furu-SEM1 (Figs 3a-b), US15.2-sc11 (Fig.

321   3c), and Furu-sc2 (Figs 3d-e) were c.a. 8.1, 6.5, and 5.5 μm, respectively. Hence,

322   specimen Furu-SEM1 belongs to the large form, whilst the specimens US15.2-sc11 and

323   Furu-sc2 belong to the Intermediate form-B of (Hagino et al., 2009) (Table 2).

324   Light microscopic studies showed that calcified cells of *B. bigelowii* often have a

325   flagellum-like organ (arrows on Fig. 3), which is capable of coiling (arrow on Fig. 3c).

326   *B. bigelowii* often adhered firmly to the surface of slide glass or petridish using this

327   organ (Figs. 3d-e). This behavior of the organ suggests that it is a haptonema. Calcified

328   cells of *B. bigelowii* were non-motile. Two equal flagella were reported from motile

329   non-calcified cells of *B. bigelowii* (= *C. parkeae*) (Green and Leadbeater, 1972), but

330   have never been observed on calcified cells of *B. bigelowii*. In relation to the coccolith

331   formation, numerous calcified *B. bigelowii* cells have been observed during isolation for

332   molecular studies (Hagino et al., 2013; Hagino et al., 2009; Takano et al., 2006) and for

333   attempted culture studies, None of these have ever been observed to possess incomplete

334   pentaliths inside the cells, nor have intracellular pentaliths been recorded in any other

335   study.

336

3-3. SEM observation of cell surface structure

338   The specimen Furu-SEM-1 originally had complete 12 pentaliths (Figs 3a-b), however

339   it lost its pentaliths during preservation of the haptonema for SEM observation, and so

340   its cell surface structure was exposed (Fig. 4). SEM observation showed that the sides

341   of the individual pentaliths (white solid arrows on Fig. 4c) and the contact surface

342   between the sides of the trapezoidal segments (black solid arrows on Fig. 4c) are

343   delineated by ridges. This cell surface structure is unlike anything observed on any

344   other coccolithophore, inded typically coccolitopohre cell surfaces are smotth with on

345   trace of the coccoliths. Clearly this distinctive surface is related to the pentaliths and so

346   we will refer to it as the *pentalith-substrate,*.

347   The ridges on the pentalith-substrate between sides of pentaliths have fine grooves that

348   correspond to laminae forming the pentaliths (dashed black arrow on Fig. 4c). In

349   addition, fine wrinkles occurred on the distal surface of the pentalith-substrate (white

350   dashed double headed arrows on Fig. 4c) with the same orientation as the fine grooves

351   observed on the inner layers of pentaliths in SEM (white solid double-headed arrows on

352   Figs. 1a and b), and *c* axis of calcite of the layers (Appendix2, Kameo and Furukawa,

353   2007). The haptonema emerged from one of the inter-plate ridges of pentalith-substrate

354   (white triangle on Fig. 4b).

355

356   **3-3. TEM observation of cell structure**

357   Figure 5a shows the general appearance of one of the thin sections obtained from a *B.*

358   *bigelowii* cell. The cell is surrounded by thick pentaliths, and the distal surface of

359   pentaliths is covered with a thin black layer (black triangles), that indicates the presence

360   of a thin organic structure covering the pentaliths. The section also shows a spherical

361   body (S. in Fig. 5a) and two chloroplasts (C in Fig. 5a). Figs. 5b and 5c are close up

362   view of Fig 5a, showing details of the organic structure. Relatively thick organic

363   structures were visible at contact surfaces between pentaliths (white solid arrows on

364   Figs. 5b-c) as well as at contact surfaces between trapezoidal segments consisting a

365   coccolith (a black solid arrow on Fig. 5b). These structures correspond to the ridges of

366   pentalith-substrate observed in SEM (black and white arrows on Fig. 4). The organic

367   structure covering distal surface of pentaliths (black triangles on Fig. 5a) consists of

368 multiple very thin layers (black triangles on Fig. 5c), and those layers were connected to

369 the ridges of pentalith-substrate (a white solid arrow on Fig. 5c). Thus, the trapezoidal

370 segments forming a pentalith are surrounded by an organic structure consisting of the

371 pentalith-substrate and thin distal organic layers.

372

373 **3-4. Crystallographic study of pentaliths**

374 TEM studies of the thin-foil section prepared from middle part of layers showed (Fig.

375 6a) that the layers consist of many elongated calcite grains, which were consistently

376 aligned (Figs 6b-c). The directions of elongation were essentially the same as those of

377 the fine grooves observed on pentaliths in SEM (double-headed white arrows on Figs

378 1a-b) (Plate 2-6 of (Hagino et al., 2009), and of the wrinkles observed on the

379 pentalith-substrate (dashed double-headed white arrows on Fig 4c). The whole area of a

380 segment (Fig. 6c) showed a sharp SAED pattern of calcite along the [21-1] zone axis

381 (Fig. 6d). This result shows all of the elongated grains in a segment have exactly the

382 same crystallographic orientations. The c-axis was not detected from the plane of this

383 thin section.

384

385 **3-5. Elemental analyses of pentaliths**

386 A total of twenty six pentaliths of *B. bigelowii*, eight heterococcoliths of *Emiliania*

387 *huxleyi*, five heterococcoliths of *Gephyrocapsa oceanica* and six heterococcoliths of

388 *Tergestiella adriatica* were examined by SEM-EDS (Fig. 7). The integrated counts of

389 Ca-Kα and Mg-Kα peaks in each spectrum were obtained. Ca and Mg counts taken

390 from the carbon tape without coccolithophores (background) were mostly lower than

391 10,000 and 800, respectively. The Ca counts ranging from ca 14,000 to 90,000 in the

392 heterococcoliths, and 40,000 to 80,000 in pentaliths of *B. bigelowii*. The Mg counts of

393 heterococcoliths were usually less than 1,000, although the counts of two coccoliths of

394 *G. oceanica* exceeded 1,000. The Mg counts of pentaliths of *B. bigelowii* ranged from

395 ca. 28,000 to 78,000, and were positively correlated with the Ca counts (R = 0.67).

396

397 **4. Discussion**

398 **4-1. Ploidy state**

399   This study revealed that calcified cells of *B. bigelowii* have a haptonema, and use it for

400   adhesion to external substrata. The calcified cells are non-motile and do not have

401   flagella, unlike non-calcifying motile cells of *B. bigelowii*, which were originally

402   described as *C. parkeae* as possessing a haptonema and two flagella (Green and

403   Leadbeater, 1994). This is the first known example of haptophytes in which the

404   non-motile cells without flagella possess a haptonema.

405   Many coccolithophores change their motility and scale morphology in their life cycle.

406   Members of Nöelaerhabdaceae (Isochrysidales) are non-motile and calcifying in diploid

407   phase, and motile and non-calcifying in haploid phase. Members of the Coccolithales

408   are non-motile and calcifying in diploid phase, and motile and calcifying in haploid

409   phase. Members of the Syracosphaerales and Zygodiscales are motile and calcifying in

410   both the diploid and haploid phases (e.g. Houdan et al., 2004; Young et al., 2003). So

411   far as is known, all haploid cells of coccolithophores are motile. The ploidy state of

412   non-motile (calcifying) and motile (non-calcifying) cells of *B. bigelowii* is still

413   unknown due to lack of culture strains, however, comparison of its behavior with that of

414   other coccolithophores suggests that the non-motile (calcifying) and motile

415 (non-calcifying) stages of *B. bigelowii* likely correspond to diploid and haploid phases,

416 respectively.

417

418 **4-2. Pentalith-substrate**

419 In this study, the presence of pentalith-substrate of the specimen Furu-SEM1 was

420 revealed as a result of dissolution of pentaliths during cleaning of the cell using

421 ion-exchanged water after fixation of the organic structure by osmium tetroxide. In our

422 experience, coccoliths/pentaliths can be dissolved in ion-exchanged water, probably

423 because ion-exchanged water is depleted in ions and the carbon dioxide in the

424 atmosphere easily dissolves in the ion-exchanged water. Another example of dissolution

425 of pentaliths in ion-exchanged water is shown in Appendix 3. The pH of the

426 ion-exchanged water used for cleaning of the specimen Furu-SEM1 is unknown, but

427 probably it was slightly acidic. (Hochuli, 2000) reported organic fossils, which closely

428 resemble the pentalith-substrate of *B. bigelowii*, from Oligocene sediments from the

429 North Sea prepared for palynological studies using hydrochloric and hydrofluoric acids.

430 The material forming the pentalith-substrate is unknown, however, observation by

431 (Hochuli, 2000) indicates that it is probably formed with some resistant

432 non-hydrolyzable biopolymer. At this moment, there are no reports on cell covering

433 formed with resistant non-hydrolyzable biopolymer from the members of the

434 Haptophytes. Therefore, it is difficult to assume the composition of pentalith-substrate

435 at this point.

436 The morphological similarity between the organic cell covering structure

437 (pentalith-substrate and thin layers) and the pentaliths of *B. bigelowii* is unusual for

438 coccolithophores. Previous studies showed that diploid cells of typical coccolithophores

439 bearing heterococcoliths have smooth cell membranes, and that there is no relationship

440 between the morphology of the cell membrane and of heterococcoliths (e.g. Drescher et

441 al., 2012; Probert et al., 2007). Haploid cells of typical coccolithophores (e.g. *C.*

442 *pelagicus*) have complex cell coverings consisting of the plasmalemma, columnar

443 material, several layers of scales, holococcoliths and an outermost investment called the

444 envelope. The organic 'envelope' is considered as delimiting the site for calcification of

445 holococcoliths (Rowson et al., 1986), but again there is no morphological similarity

446 between cell membrane structure and holococcoliths. As we reported above, trapezoidal

447   segments of pentalith of *B. bigelowii* are surrounded by the pentalith-substrate and

448   multiple very thin organic layers. The site for calcification of the pentaliths has not been

449   confirmed yet due to the lack of in situ observations of calcification, however, the close

450   morphological similarities suggest that the organic pentalith-substrate and thin layers

451   may act as a 'guide' for the shaping of pentaliths, and the organic layers covering distal

452   side of trapezoidal segment may correspond to 'envelope' of motile cells of *C.*

453   *pelagicus*.

454

455   **4-3. Process of calcification**

456   A pentalith with incomplete calcareous layers (Fig. 2e) can be considered as in the

457   process of calcification or malformation rather than the result of secondary dissolution

458   of layers, since secondary dissolution of pentalith starts from the margin of pentaliths

459   not from the center of pentaliths (Appendix 3). Presence of multiple incomplete

460   calcified layers along ridges of pentalith-substrate suggests that *B. bigelowii* calcify

461   multiple layers at the same time (arrow on Fig. 2e).

462   A naked cell without pentaliths but with pentagonal impressions on its cell surface,

463   which resembles the pentalith-substrate of *B. bigelowii*, was observed in this study (Fig.

464   2f). The sample, which yielded the naked cell, also contained many *B. bigelowii* cells

465   with calcified pentaliths. Therefore, if it is *B. bigelowii,* it should be in the state prior to

466   the start of calcification rather than a cell that lost pentaliths due to secondary

467   dissolution. If the cell is in the precursor state to calcification, presence of twelve

468   impressions of pentaliths on a cell (Fig. 2f) suggest that *B. bigelowii* does calcification

469   of 12 pentaliths on cell surface synchronously.

470   We have isolated > 500 of cells of *B. bigelowii* through our previous studies and

471   on-going culture studies, but never seen incomplete pentaliths within the cell of *B.*

472   *bigelowii* (Hagino et al., 2013; Hagino et al., 2009; Takano et al., 2006) (personal

473   observation by KH). The lack of observation of incomplete pentaliths inside the cell

474   supports our hypothesis that *B. bigelowii* calcifies the 12 pentaliths synchronously on its

475   cell surface not inside the cell.

476

477   **4-3. Mineralogical characteristics of pentaliths**

478   TEM study of a pentalith revealed that the layers in the thin-foil section consist of

479   numerous calcite grains elongated in almost the same direction (Figs 6b-c). Since the

480   thin-foil section was prepared from intermediate part of layers, which is hardly affected

481   by secondary-dissolution, the morphology observed in TEM is a primary structure not

482   the result of dissolution. The direction of the long axis of the grains and their

483   appearance looks to be the same as that of the fine grooves observed from inner layers,

484   which were exposed by loss of the outermost smooth distal layer (double-headed solid

485   arrows in Figs 2a-b) (Fig. 2-6 of Hagino et al., 2009). The similarity in structure

486   observed in both TEM and SEM suggests that the fine grooves observed by loss of

487   outermost layers are also a primary structure. This result raised another question, why

488   does the only outermost distal layer have a smooth surface? The absence of fine

489   grooves/calcite grain structure can be explained by multiple organic layers covering the

490   distal surface of pentalith (black triangles on Fig. 5c) that may conceal the fine structure

491   of distal lamina.

492   The direction of the long axis of the calcite grains looks to be the same as that of the

493   fine wrinkles observed on the distal surface of the pentalith-substrate (double headed

494   dashed arrows on Fig. 4c). Similarity in direction of calcite grains and wrinkles of

495   pentalith-substrate suggest a possibility: the pentalith-substrate plays a role on growth

496   of calcite grains.

497   The examined TEM section should consist of a couple of stacked lamina, since the

498   thin-foil TEM section (c.a. 180 nm) was much thicker than that of a single lamina of the

499   pentalith (< 70 nm, Appendix 4). Therefore, calcite grains in all the lamina have

500   perfectly identical crystal orientation. This suggests that *B. bigelowii* strictly controls

501   crystal orientation of calcite grains.

502

503   **4-4. Chemical contents of pentaliths**

504   Heterococcoliths calcified intracellularly contain very low Mg^{2+} (1/10~ 1/100) in

505   comparison to foraminiferan tests calcified extracellularly (Stoll et al. 2001). That is

506   consistent with the highly regulated selective ion transport mechanism utilized during

507   calcification (Brownlee and Taylor, 2004; Stoll and Ziveri, 2004). On the other hand,

508   holococcoliths, which are calcified outside the periplast (Rowson et al., 1986), contain

509   higher amount of Mg than heterococcoliths (Cros et al., 2013). Our study revealed that

510   *B. bigelowii* almost certainly calcifies pentaliths extracellularly, and always contain a

511   relatively high amount of Mg in the pentalith. Together with the results from (Cros et al.,

512   2013), our study showed that elemental compositions of calcified scales are correlated

513   with the site of calcification, and that higher contents of Mg in the calcified scales

514   indicates extracellular calcification. The phylogenetic positions and the sites of

515   calcification of many other nannolith-bearing species, such as *Nannoconus*, are still

516   unknown. So, elemental studies of calcareous nannofossils using EDS would be useful

517   to help identify the calcification sites as well as understanding of phylogeny of extinct

518   calcareous nannofossils.

519   Elemental compositions of foraminiferan tests have been used for reconstruction of the

520   temperature and/or water chemistry in geological ages (e.g. Barker et al., 2005). The

521   high Mg content of pentaliths of *B. bigelowii* suggests the possibility that pentaliths will

522   record seawater chemistry at the time of the calcification as is the case for foraminiferan

523   tests. The fossil records of the family Braarudosphaeraceae extend back to the Early

524   Cretaceous (140 million years ago) with no change in ulstrastructure, (Bown, 1998). So,

525   we predict that pentaliths of the Braarudosphaeraceae may provide valuable records of

526   the chemical conditions of seawater in the geological past.

527

528   **5. Summary**

529   1.   Non-motile calcified cells of *Braarudosphaera bigelowii* do have a haptonema but

530   do not possess flagella. *B. bigelowii* uses the haptonema for adhesion to external

531   substrates.

532   2.   *B. bigelowii* has a pentalith-substrate that closely underlies the calcareous

533   pentaliths, and multiple organic thin layers that develop from ridges of the

534   pentalith-substrate extend onto the distal surface of the pentaliths. The close

535   morphological correspondence suggests that the pentalith-substrate and organic

536   thin layers act as a 'guide' for shaping the pentaliths, and for calcification of 12

537   pentaliths covering a cell occur on pentalith-substrate at the same time.

538   3.   *Braarudosphaera* pentaliths consistently show higher Mg content than regular

539   heterococcoliths, closer to the values, which would be expected for equilibrium

540   calcification from sea-water. This supports our hypothesis that *B. bigelowii* calcify

541   their pentaliths extracellularly rather than in an intracellular compartment, it also

542   makes them of potential value for geochemical study.

543

552

553   **Figure Caption**

554   Fig. 1. Location of samples used in this study: (a) Locality of Furue, Usuka, and Tomari

555   ports. (b) Locality of sampling stations in the Tomari area.

556   Fig. 2. Scanning electron and light microscopic images of *Braarudosphaera bigelowii*

557   and SEM image of an unknown specimen, resembling *B. bigelowii*.

558   (a) *B. bigelowii* from st. 3 of Tomari Port (June 27, 2009). (b) *B. bigelowii* from st. 3 of

559   Tomari Port (June 27, 2009). (c) *B. bigelowii* from st. D of Tomari Port (June 15, 2012).

560   (c) Lightly calcified *B. bigelowii* specimen from offshore Tomari (June 17, 2013). (d)

561   Lightly calcified specimen of *B. bigelowii* from st. D of Tomari Port (June 21, 2011).

562   (e) Incomplete pentalith of *B. bigelowii* from offshore Tomari (June 17, 2013). (f)

563   unidentified cell that has *B. bigelowii*-like cell surface structure from st. 1 of Tomari

564   Port (June 21, 2010). Note. Arrow on (e) indicates position where multiple laminae are

565   visible. Double-headed arrows on (a) and (b) indicate the orientation of the grooves on

566   the laminae.

567   Fig. 3. Light microscopic images of *B. bigelowii*: (a) and (b) Specimen Furu-SEM1. (c)

568   specimen US15.2-sc11, (d) and (e) Furu-sc2. White arrows indicate the haptonema.

569   Fig. 4. SEM images of cell surface structure of the specimen Furu-SEM1. (a) general

570   view of the specimen. (b) close up view of the base of the haptonema (white triangle).

571   (c) Close up view showing the pentalith-substrate. Solid white arrows indicate

572 pentalith-substrate between contact surfaces of pentaliths. Solid black arrows indicate

573 extensions of the pentalith-substrate into the contact surface between trapezoidal

574 segments. Dashed black arrow shows horizontal lines on pentalith-substrate that

575 corresponds to laminae of pentalith. Double-headed dashed white arrows show the

576 direction of fine corrugations on the pentalith-substrate structure.

577 Fig. 5. TEM images of a cytological section through a *B. bigelowii* cell. (a) Complete

578 cytological section of the *B. bigelowii* cell. (b and c) Details of the cross section. C. and

579 S in Fig. 5(a) indicate chloroplast and spheroid body, respectively. Solid white arrows

580 indicate the pentalith-substrate extending between the pentaliths and protruding slightly

581 beyond them. Solid black arrow indicates pentalith-substrate intruding into the contact

582 surface between trapezoidal segments. Black triangles indicate thin organic layers

583 covering the distal surface of the pentalith and connected to the pentalith-substrate.

584 Fig. 6. Thin-foil cross section of pentaliths of *B. bigelowii* cut using a focused-ion beam

585 (FIB) apparatus. (a) TEM image of the whole section, this comprises a section parallel

586 to the surface of one pentalith (black arrow) and through the sides of two neighboring

587 pentaliths (white arrows). (b) Close up view of a segment of Fig. 6a in TEM. (c)

588 High-angle annular dark field (HAADF) image of the segment in Fig. 6b, showing a

589 skeletal texture consisting of elongated calcite grains. The contrast is mainly caused by

590 averaged atomic numbers of the sample. Bright area shows elongated calcite grains. The

591 direction of the elongation corresponds to that of fine graves in SEM observation (Figs.

592 2a and b). (d) Electron diffraction pattern taken from whole area of the segment b along

593 the [21-1] zone axis. The pattern shows all of the elongated grains have exactly same

594 crystallographic orientations.

595 Fig. 7. Mg and Ca X-ray microanalysis counts for pentaliths of *B. bigelowii,*

596 heterococcoliths of *Emiliania huxleyi*, *Gephyrocapsa oceanica*, and *Tergestiella*

597 *adriatica*, and background.

598

599 **Reference**

600 Barker, S., Cacho, I., Benway, H., Tachikawa, K., 2005. Planktonic foraminiferal
601 Mg/Ca as a proxy for past oceanic temperatures: a methodological overview and data
602 compilation for the Last Glacial Maximum. Quaternary Sci. Rev. 24, 821-834.

603 Bown, P.R., 1998. Calcareous nannofossil biostratigraphy. Kluwer Academic
604 Publishers, London.

605 Bown, P.R., Lees, J.A., Young, J.R., 2004. Calcareous nannoplankton evolution and
606 diversity through time, in: Thierstein, H.R., Young, J.R. (Eds.), Coccolithophores -

607   From molecular processes to global impact. Springer, Berlin Heidelberg New York, pp.
608   481-508.

609   Brownlee, C., Taylor, A., 2004. Calcification in coccolithophores: A cellular
610   perspective in: Thierstein, H.R., Young, J.R. (Eds.), Coccolithophores - From molecular
611   processes to global impact. Springer, Berlin Heidelberg New York, pp. 31-49.

612   Cros, L., Fortuño, J.-M., Estrada, M., 2013. Elemental composition of coccoliths:
613   Mg/Ca relationships. Scientia Marina 77, 1-5.

614   de Vargas, C., Aubry, M.-P., Probert, I., Young, J.R., 2007. Origin and evolution of
615   coccolithophores: From coastal hunters to oceanic farmers, in: Falkowski, P.G., Knoll,
616   A.H. (Eds.), Evolution of Primary Producers in the Sea. Elsevier, Boston, pp. 251-285.

617   Drescher, B., Dillaman, R.M., Taylor, A.R., 2012. Coccolithogenesis In *Scyphosphaera*
618   *apsteinii* (Prymnesiophyceae). J. Phycol 48, 1343–1361.

619   Edvardsen, B., Wenche, E., Throndsen, J., G. Sáez, A., Probert, I., Medlin, L.K., 2011.
620   Ribosomal DNA phylogenies and a morphological revision provide the basis for a
621   revised taxonomy of the Prymnesiales (Haptophyta) Eur. J. Phycol. 46, 202-228.

622   Green, J.C., Hori, T., 1994. Flagella and flagellar roots, in: Green, J.C., Leadbeater,
623   B.S.C. (Eds.), The Haptophyte Algae. Clarendon Press, Oxford, pp. 47-71.

624   Green, J.C., Leadbeater, B.S.C., 1972. *Chrysochromulina parkeae* sp. nov.
625   [Haptophyceae] a new species recorded from S.W. England and Norway. J. mar. biol.
626   Ass. U. K. 52, 469-474.

627   Green, J.C., Leadbeater, B.S.C., 1994. The Haptophyte Algae, Systematics Association
628   Special Volumes. Clarendon Press, Oxford, p. 446.

629   Hagino, K., Onuma, R., Kawachi, M., Horiguchi, T., 2013. Discovery of an
630   endosymbiotic nitrogen-fixing cyanobacterium UCYN-A in *Braarudosphaera bigelowii*
631   (Prymnesiophyceae). PLoS One 8, e81749.

632   Hagino, K., Takano, Y., Horiguchi, T., 2009. Pseudo-cryptic speciation in
633   *Braarudosphaera bigelowii* (Gran and Braarud) Deflandre. Mar Micropaleontol 72,

634   210-221.

635   Hagino, K., Young, J.R., Bown, P.R., Godrijan, J., Kulhanek, D.K., Kogame, K.,
636   Horiguchi, T., 2015. Re-discovery of a "living fossil" coccolithophore from the coastal
637   waters of Japan and Croatia. Mar. Micropaleontol. 116, 28-37.

638   Hochuli, P.A., 2000. 'Organic nannofossils': a new type of palynomorph from the
639   Palaeogene of the North Sea. J. Micropal. 19, 153-158.

640   Houdan, A., Billard, C., Marie, D., Not, F., Sáez, A.G., Young, J.R., Probert, I., 2004.
641   Holococcolithophore-heterococcolithophore (Haptophyta) life cycles: flow cytometric
642   analysis of relative ploidy levels. Systematics and Biodiversity 1, 453-465.

643   Inouye, I., Kawachi, M., 1994. The haptonema, in: Green, J.C., Leadbeater, B.S.C.
644   (Eds.), The Haptophyte Algae. Clarendon Press, Oxford, pp. 73-89.

645   Kameo, K., Furukawa, N., 2007. Analysis of crystallographic directions in Florisphaera
646   profunda, Braarudosphaera bigelowii and Neogene discoasters: preliminary report on
647   nannolith crystallography. J. nannoplankton Res. 29, 19-23.

648   Kawachi, M., Inouye, I., Maeda, O., Chihara, M., 1991. The haptonema as a
649   food-capturing device: observations on *Chrysochromulina hirta* (Prymnesiophyceae).
650   Phycologia 30, 563-573.

651   Medlin, L.K., Sáez, A.G., Young, J.R., 2008. A molecular clock for coccolithophores
652   and implications for selectivity of phytoplankton extinctions across the K/T boundary.
653   Mar Micropaleontol 67, 69-86.

654   Perch-Nielsen, K., 1985a. Cenozoic calcareous nannofossils, in: Bolli, H.M., Saunders,
655   J.B., Perch-Nielsen, K. (Eds.), Plankton Stratigraphy. Cambridge University Press,
656   Cambridge, pp. 427-555.

657   Perch-Nielsen, K., 1985b. Mesozoic calcareous nannofossils, in: Bolli, H.M., Saunders,
658   J.B., Perch-Nielsen, K. (Eds.), Plankton Stratigraphy. Cambridge University Press,
659   Cambridge, pp. 329-426.

660   Probert, I., Fresnel, J., Billard, C., Geisen, M., Young, J.R., 2007. Light and electron

661   microscope observations of *Algirosphaera robusta* (Pymnesiophyceae). J. Phycol. 43,
662   319-332.

663   Rowson, J.D., Leadbeater, B.S.C., Green, J.C., 1986. Calcium carbonate deposition in
664   the motile (*Crystallolithus*) phase of *Coccolithus pelagicus* (Prymnesiophyceae). Br.
665   phycol. J. 21, 359-370.

666   Stoll, H.M., Ziveri, P., 2004. Coccolithophorid-based geochemical paleoproxies, in:
667   Thierstein, H.R., Young, J.R. (Eds.), Coccolithophores - From molecular processes to
668   global impact. Springer, Berlin Heidelberg New York, pp. 529-561.

669   Takano, Y., Hagino, K., Tanaka, Y., Horiguchi, T., Okada, H., 2006. Phylogenetic
670   affinities of an enigmatic nannoplankton, *Braarudosphaera bigelowii* based on the SSU
671   rDNA sequences. Mar Micropaleontol 60, 145-156.

672   Thompson, A.W., Foster, R.A., Krupke, A., Carter, B.J., Musat, N., Vaulot, D.,
673   Kuypers, M.M.M., Zehr, J.P., 2012. Unicellular Cyanobacterium Symbiotic with a
674   Single-Celled Eukaryotic Alga. Science 337, 1546-1550.

675   Tsutsui, K., Kumon, H., Ichikawa, H., Tawara, J., 1976. Preparative method for
676   suspended biological materials for SEM by using polycationic substance layer. J.
677   Electron Microsc. 25, 163-168.

678   Westbroek, P., Young, J.R., Linschooten, K., 1989. Coccolith production
679   (Biomineralization) in the marine alga *Emiliania huxleyi*. J. Protozool. 36, 368-373.

680   Young, J.R., Davis, S.A., Bown, P.R., Mann, S., 1999. Coccolith ultrastructure and
681   biomineralisation. J. struct. Biol. 126, 195-215.

682   Young, J.R., Geisen, M., Cros, L., Kleijne, A., Probert, I., Ostergaard, J.B., 2003. A
683   guide to extant coccolithophore taxonomy. J Nannoplankton Res, Special Issue 1,
684   1-132.

685

a

Sea of Japan

Tomari Tottori

Usuka
Furue

Pacific Ocean

45°N

40°N

35°N

30°N

130°E   135°E   140°E   145°E

b

offshore
samples

100 m

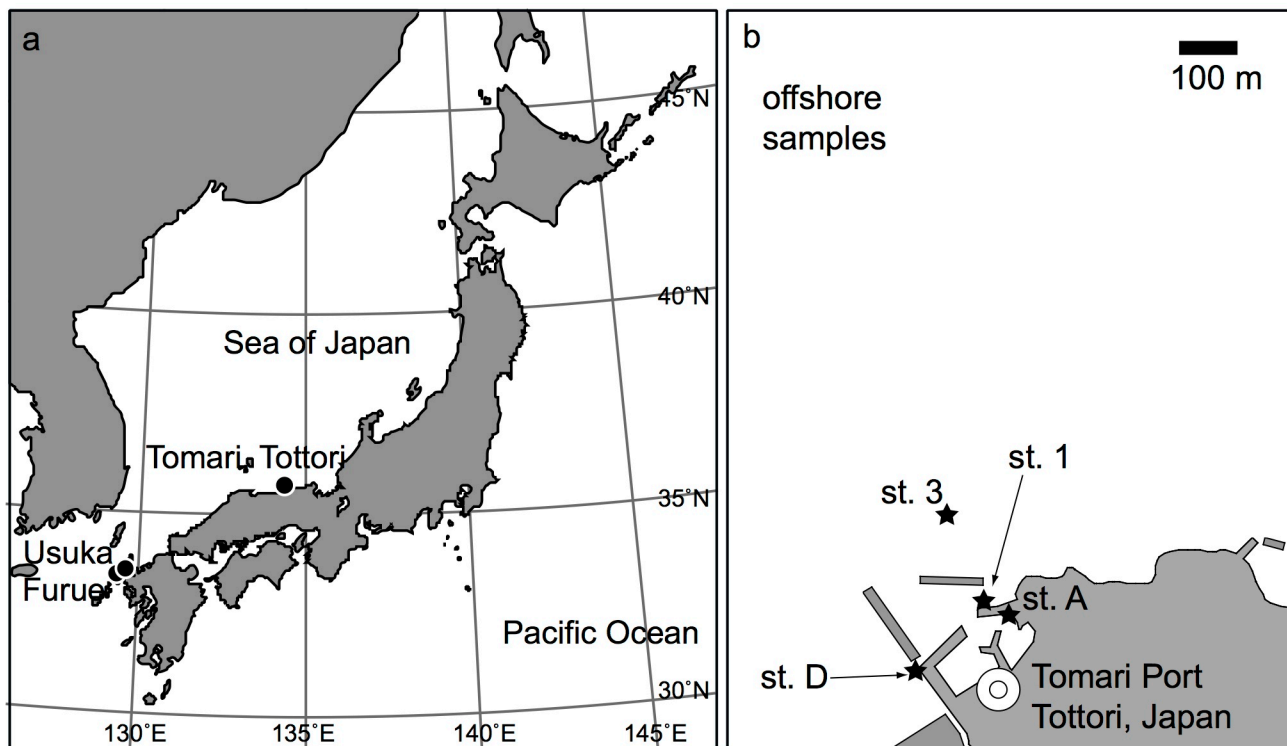st. 3

st. 1

st. A

st. D

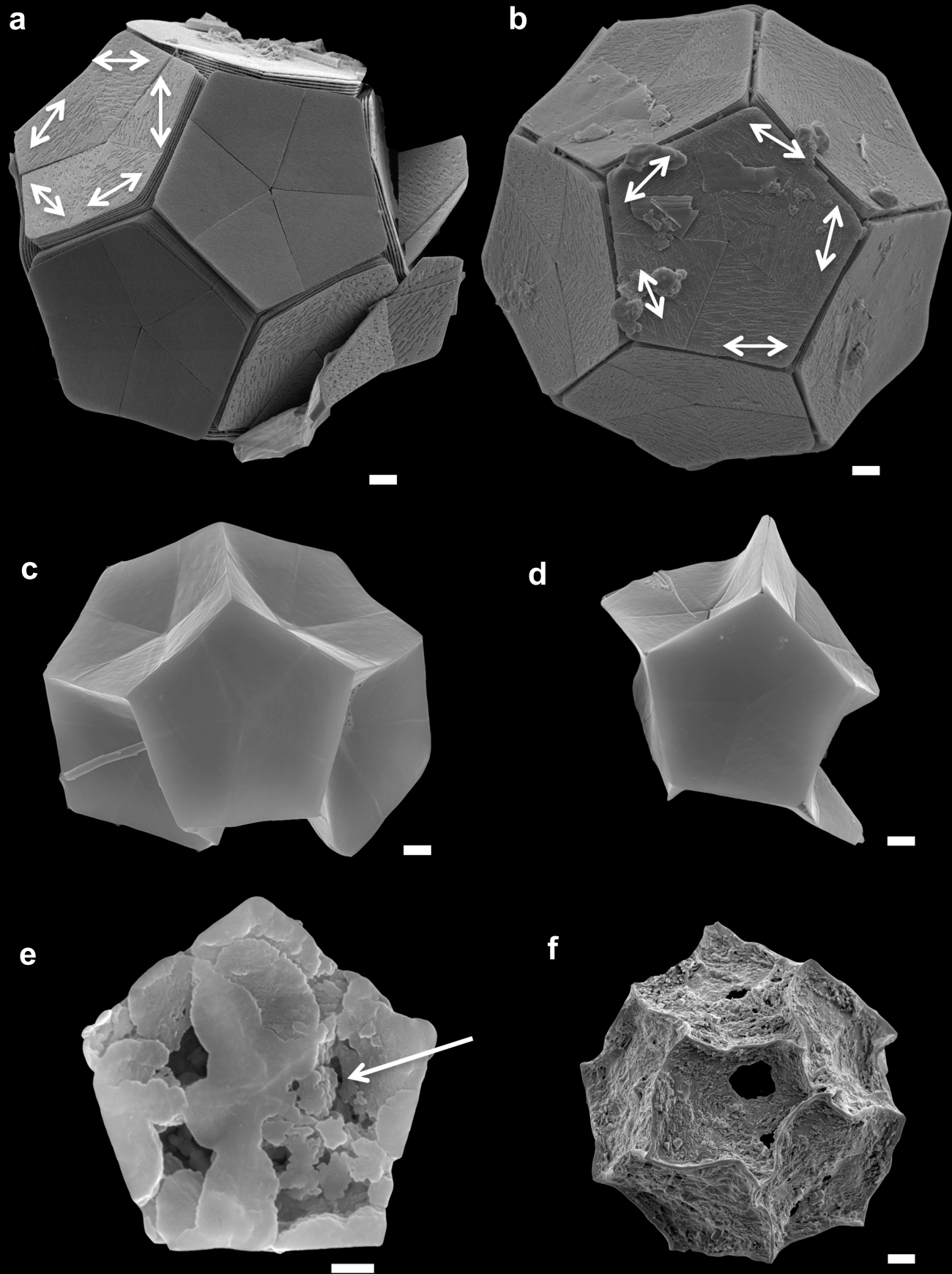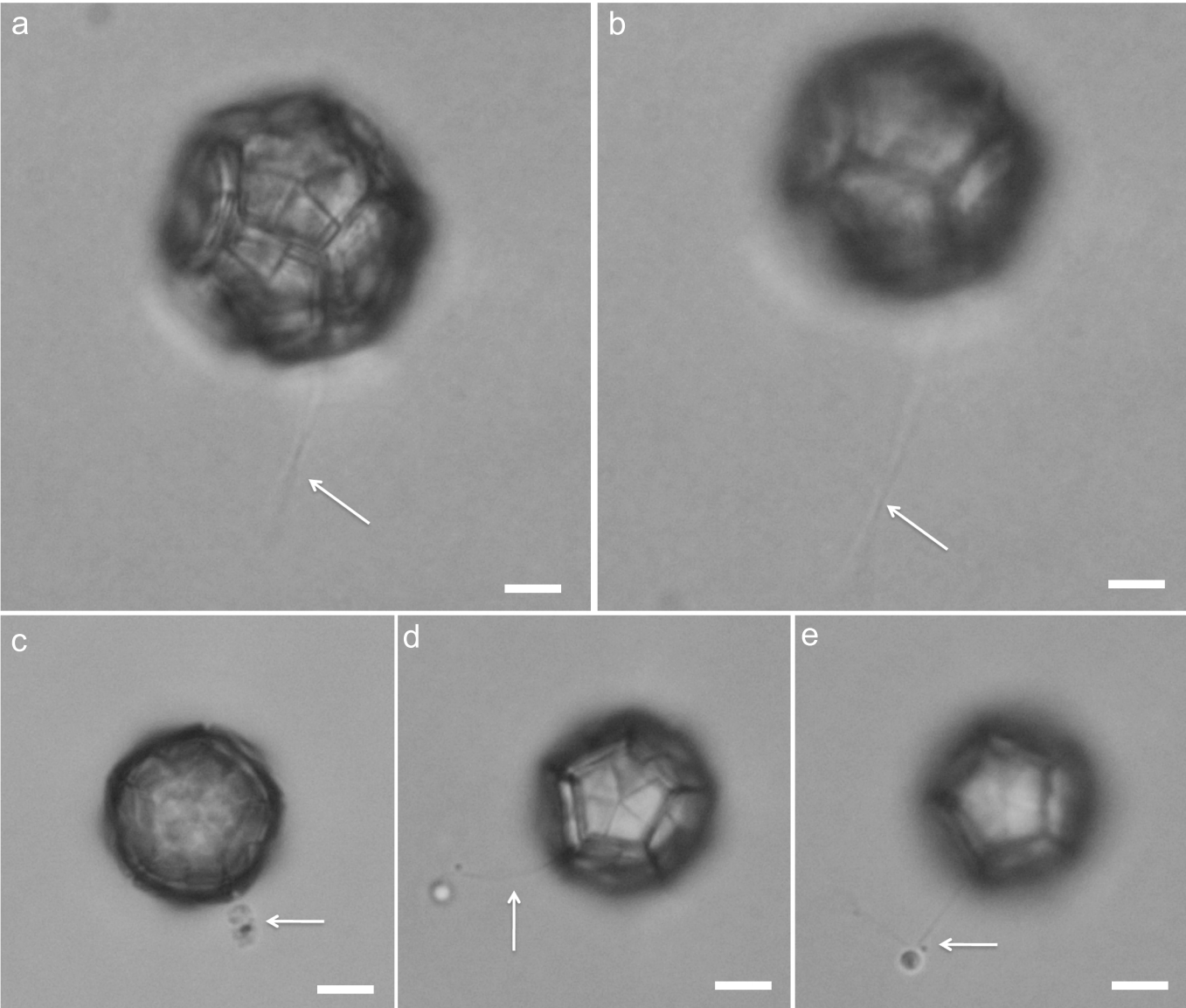Tomari Port
Tottori, Japan

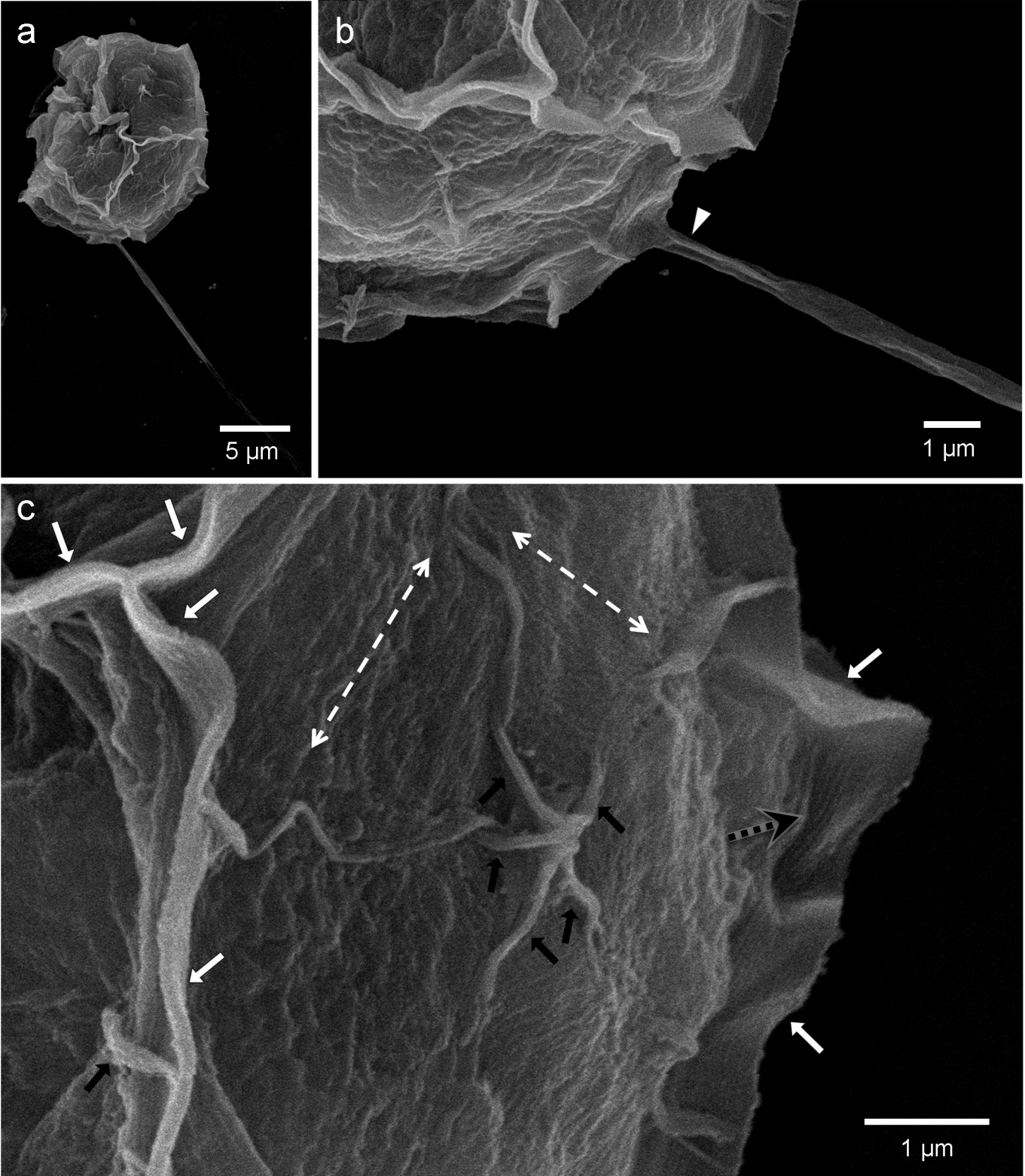Fig. 1 Hagino et al.

Fig. 2 Hagino et al.
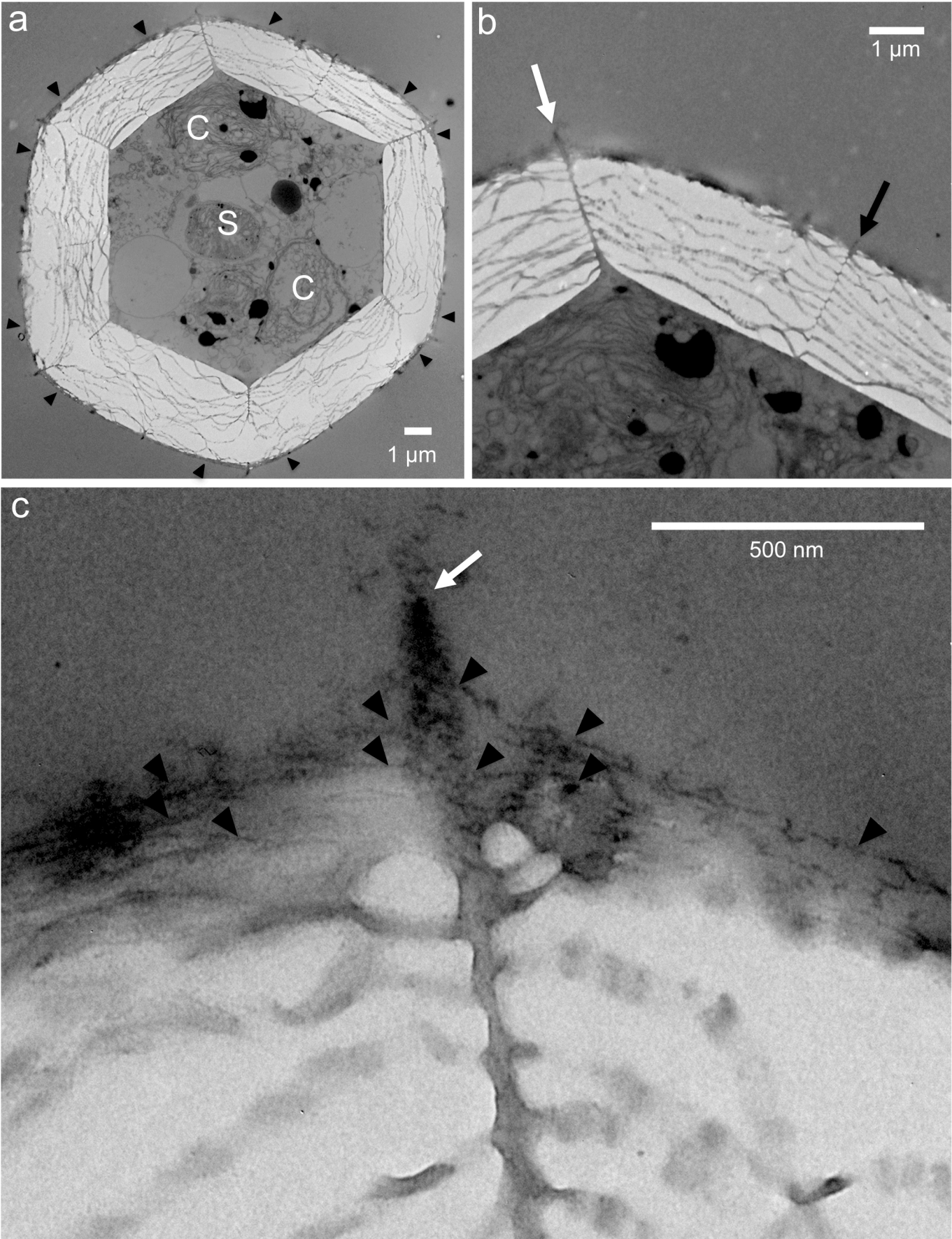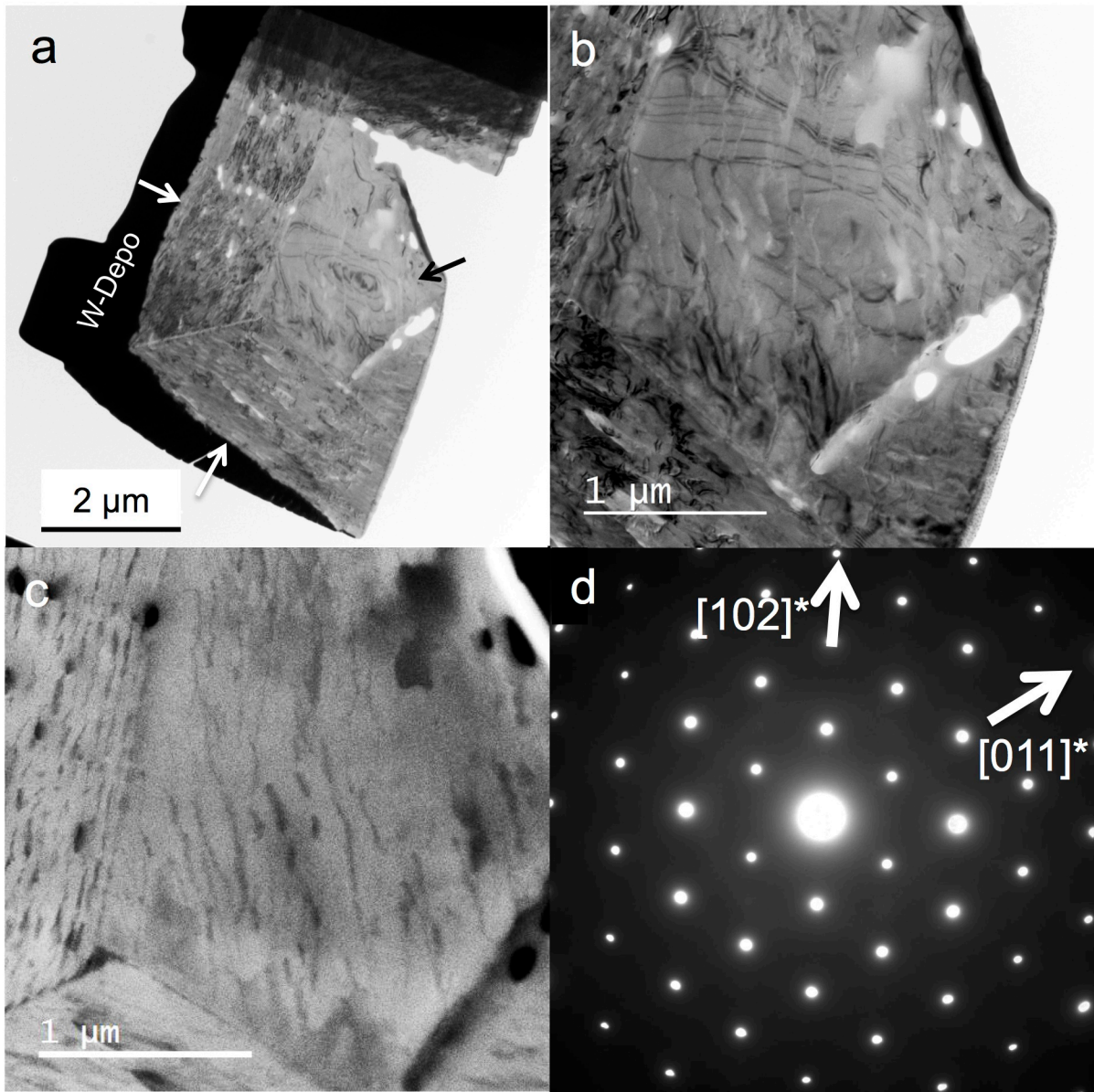
Fig. 3 Hagino et al.

Fig. 4 Hagino et al.

Fig. 5 Hagino et al.

Fig. 6. Hagino et al.

Fig. 7, Hagino et al.